

ANALYSIS OF LOW ENERGY PION TEST BEAM DATA GIVING THE COMBINED RESPONSE OF THE ELECTROMAGNETIC AND HADRONIC CALORIMETERS

F. Combley, M. Dinsdale, M. Pepe, M. de Palma, L. Silvestris

1 Introduction

This report gives the results of the analysis of pion data taken in the spring of 1988 in the West Area test beam with an ECAL end-cap in combination with the HCAL prototype[1]. Data taken in 1987 at beam energies between 5 and 30 GeV has been extended by the 1988 data which focused on the low energy range below 10 GeV. Analysis of the 1987 data showed that the resolution of the combined calorimeter improved at lower energies and was broadly consistent with the value for HCAL alone at higher energies [2]. The 1988 data taken at 10, 7.5, 3, 2 GeV pion beams allowed a more complete investigation of the combined response of the two calorimeters at lower energies. Results from the analysis of this new data and where possible a comparison with that of 1987 are given below.

2 ALEPH Test Beam

Measurements were carried out in the ALEPH test zone situated in the X7 beam line in the West Area at CERN. The detector arrangement is shown in figure 1 and was identical to that used in 1987. The calorimeters were configured so that the beam was at 30° to normal incidence. The full 5 x 5 array of HCAL towers was read out while ECAL signals from a zone of 276 towers were recorded.

The beam line itself was upgraded especially for this data taking period. In order to obtain a reasonable pion flux at as low an energy as 2 GeV, magnets were exchanged for ones more stable at low currents, two extra quadrupoles were added and the beam path was cleared of all surplus absorbing material. This latter included the removal of one of the two gas filled Cerenkov detectors and the extension of the beam vacuum pipe as far as possible into the ALEPH area itself.

A telescope of five scintillation counters (T1 to T5 in Figure 1) together with the single beam Cerenkov detector were used to define particle type. The two final scintillation counters were placed downstream of the calorimeters and muon chambers behind 40 cm of iron and were used to signal muons while the Cerenkov detector was used to differentiate between electrons and pions or muons. Muons in the beam which did not pass through the final two scintillators were identified by use of the muon chambers and the digital pattern signal of HCAL. Finally information from the spectrometer multiwire chambers and the Saclay chambers in the test zone were recorded and used to select events with a single unambiguous beam particle.

At regular intervals throughout the data taking period, separate electron runs with a 10 GeV beam were made in order to calibrate the ECAL. The HCAL calibration was achieved from dedicated pion beam runs without ECAL in front.

3 Definition of the Data Sample

Information from four spectrometer multiwire chambers, two upstream and two downstream of the magnet, were used to identify events with a clean beam track. After correlation cuts to remove stray hits in the chambers, only events with a single hit in all four chambers were accepted. The two correlation cuts were based, one on a correlation between hits in the two downstream chambers and the other on the basis of ingoing and outgoing tracks matching.

In addition, two Saclay chambers located close to the calorimeters (Figure 1b) were used to identify events with a clean beam track. Cuts based on the correlation between the coordinates given by these two chambers were used in order to remove particles which were clearly outside the beam phase space. However even after these cuts a large number of events still contained multiple hits and so events with one hit in one chamber and two in the other were accepted in addition to those with single hits throughout. The former were accepted under a separate flag [IYES = 1] and were considered to be due to a single particle plus sparking wire. The extent to which the data sample is reduced by these beam cuts is shown in Table 1.

For about 5% of the events at 2GeV it was not possible to distinguish pions from muons which stopped in the HCAL. These events failed to produce a signal in the muon chambers and the digital pattern signal did not clearly indicate that an interaction had occurred. These events were flagged and not included in the pion analysis.

Within the pion data sample which passed all the beam cuts there were two types of events which had to be removed from the analysis. One type arose from a problem with the data acquisition which resulted in an occasional event being written out twice. The second type was more significant and came from a small number of events (approximately 0.2%) in which all ECAL towers in stack 2 were above threshold. This compares with an average event in which approximately fifteen towers above threshold are summed to obtain the total energy deposited in ECAL. On analysis these particular events were found to carry a total negative energy in ECAL which was of the order -300.0 GeV coming from -400.0 in both stack 1 and 3 and $+500.0$ in stack 2. Such signals can only be attributed to a systematic shift in the pedestals which could result, for example, from a spark in the ECAL module. A simple cut on the number of towers above threshold removed these events from the analysis.

Contamination of the pion sample by electrons can be studied by making a cut on the ratio of the energy in the four towers with the four highest energies in ECAL divided by the beam energy. Events with a ratio greater than 0.75 are consistent with electrons in the pion sample. This technique selected 1 to 2% of the pions as electrons but on examination of their wire profiles it was obvious that a large

Table 1: Test beam data before and after beam cuts

Energy	Total	Before beam cuts		After beam cuts	
		Pions	Muons	Pions	Muons
10GeV	7.64K	6.44K	1.20K	4.78K	0.45K
7GeV	18.67K	15.92K	2.75K	10.70K	0.97K
5GeV	8.26K	6.99K	1.27K [IYES = 1]	4.35K 5.35K	0.33K 0.68K
3GeV	7.18K	5.78K	1.40K	2.66K 4.01K	0.25K 0.54K
2GeV	11.48K	7.55K	3.93K	1.94K 3.93K	0.12K 0.27K

fraction of these events were pions showering in the third stack and only 10% of those identified were actually electrons. Thus the electron contamination of the sample was less than 0.2%. This method is similar to that proposed as part of the electron identification package in the reconstruction program JULIA.

Before proceeding to discuss the energy resolution obtained in the present analysis it should be noted that there is an important difference between this and the earlier work[2]. This difference is to do with the so called zero suppression energy threshold used on the ECAL storeys. Signals from an ECAL tower are not included in the energy sum unless the individual signal from at least one of its storeys exceeds the threshold. In the 1987 analysis this threshold was set at 16MeV but subsequent studies of electron data showed that at low energy both the resolution and linearity were affected by the choice of threshold. With a value of 16MeV the energy resolution deteriorates significantly at low energy due to noise (Figure 2) while at 50MeV threshold the linearity is poorer because signal loss becomes more significant in this region. These two considerations led to a choice of 32MeV and in order to make a proper comparison the analysis of the 1987 data was redone with this value. As can be seen below this latter does not change the conclusions drawn from that earlier study.

4 Energy Resolution and e/π ratio

The ECAL was calibrated using 10GeV electrons and the HCAL calibrated using pions so that in combining the energies from the two calorimeters each

component is weighted by a coefficient to reflect their different response and their different calibration. In this analysis we combine stacks 1 and 2 of ECAL as they are identical in construction but attach a separate coefficient to stack 3, so that the energy measured is expressed as

$$E_t^i = k_1(E_1^i + E_2^i) + k_2E_3^i + k_3H^i$$

where k_1, k_2, k_3 , are coefficients to be determined and E_1^i, E_2^i, E_3^i are the energies in the three stacks of ECAL and H^i is the energy contained in HCAL for event i . With a constraint on the mean equalling the beam energy, the three coefficients were adjusted to minimise the spread in energies for the pion sample. Thus we minimised

$$\sigma = \sqrt{\sum_i (E_t^i - E_{\text{beam}})^2}$$

with the constraint

$$\langle E_t \rangle = E_{\text{beam}} = 1/N \sum_i [k_1(E_1^i + E_2^i) + k_2E_3^i + k_3H^i]$$

The resolution was minimised individually at each beam energy to illustrate, if any, the energy dependance of the coefficients.

A global minimisation of all data, including that for 1987, gave a single set of coefficients. In this case the quantity minimised is the sum over all energies

$$\sum_i (E_t^i - E_{\text{beam}})^2 / \sigma^2$$

where σ represents the spread observed at each individual energy. Because the combined resolution changes with energy the coefficients obtained depend upon the relative weights given to data at different energies. A simple procedure was followed in which equal size samples at all energies were taken but in order to check the sensitivity of this choice an alternative method in which sample sizes reflected the energy spectrum from Lund events as shown in Figure 3 was also tried. The individually minimised coefficients are shown in Figure 4 together with those from the simple global procedure and it can be seen that the former stay close to the latter at all energies with the possible exception of 2GeV. However at low energy the coefficients are not strongly determined by minimising the energy resolution. For example this latter is not significantly changed in going from the individual to the global coefficients. When the data samples in the global minimisation were weighted according to the Lund distribution the resulting coefficients produced an energy resolution at 20 and 30GeV which was worse by about 4% while leaving the values at lower energy essentially unchanged. This again points to the fact that the resolution at energies below 10GeV is relatively insensitive to the values of the coefficients.

In Figure 4 the coefficient for stack3 is systematically lower than that for stacks1,2. This is because the signals from the former are corrected for the different amount of material (4mm lead sheets instead of 2mm etc) in terms of radiation lengths. This factor is 1.92 while the different global coefficients indicate that a factor 1.68, closer to the ratio of interaction lengths, would be better.

The measured distributions after minimisation (Figure 5) are seen, especially at low energy, to have large tails and a non-gaussian shape. Gaussian fits to these distributions were inappropriate so instead a two sigma width was defined as that which contained 68% of the total area of the distribution. The energy resolution as a function of energy using individually minimised coefficients is shown in figure 6a. Figure 6b is the same plot for the single set of coefficients obtained from the global minimisation with equal data samples. For this latter case the linearity of the energy measurement is shown in Figure 7.

A measure of the e/π ratio can be obtained from the coefficient for ECAL stacks 1,2 when the HCAL coefficient, k_3 , is set to one. With this constraint on k_3 , the HCAL is used at its correct hadron calibration so that the ECAL coefficients represent the relative response of the calorimeter to hadronic showers. The variation of the e/π ratio as a function of energy is shown in figure 8.

The average fraction of the total pion energy which is deposited in ECAL according to the global coefficients is shown in Figure 9.

5 Effect of the coil

Test beam data was also taken with the first plane of HCAL switched off to assess the effect of the material of the superconducting coil on the resolution. The resolution when simulating the presence of the coil material is seen to worsen by some 6% at high energy but at low energy this is as little as 2% (Figure 10a). Finally in Figure 10b the linearity in the energy measurement is shown when only one set of coefficients is used for the data where the coil is simulated.

References

[1] A full description of the HCAL prototype can be found in
MG Catanesi et al : NIM A247,438(1986)

[2] M de Palma, M Pepe, G Raso, M-N Minard, F Combley: ALEPH note 88-10

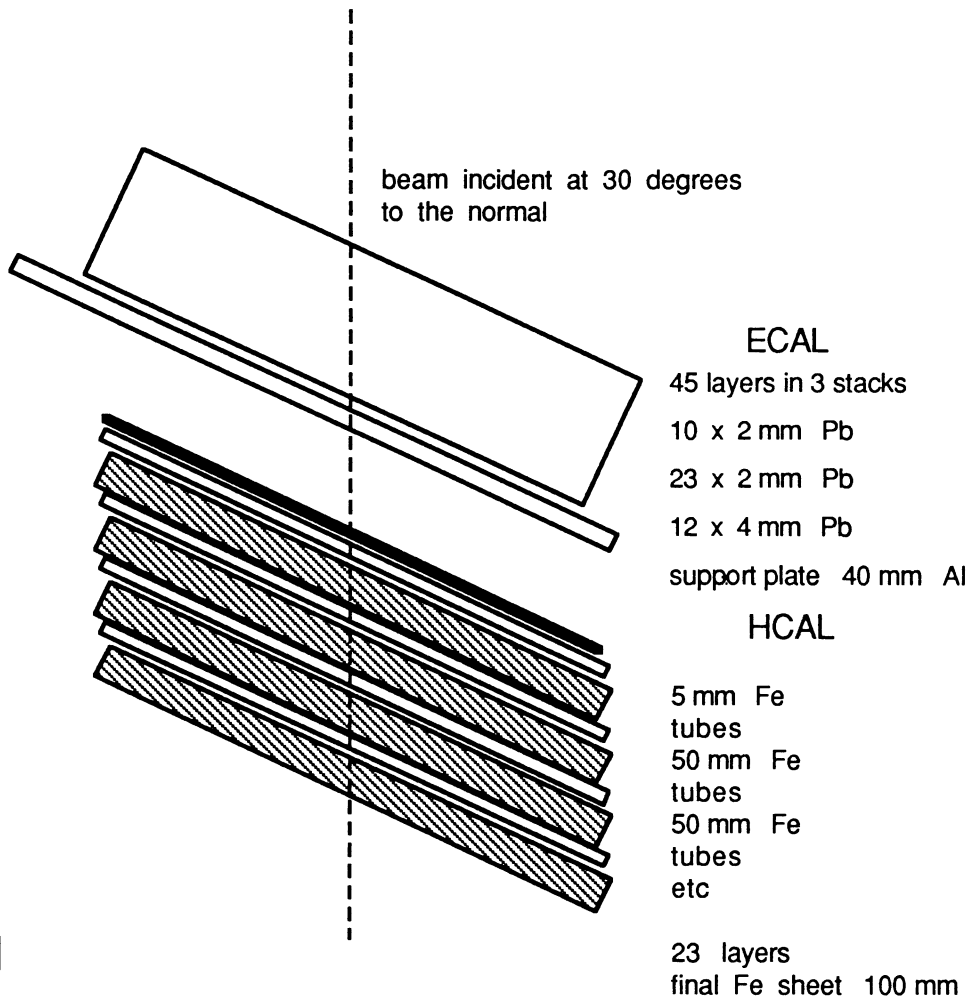
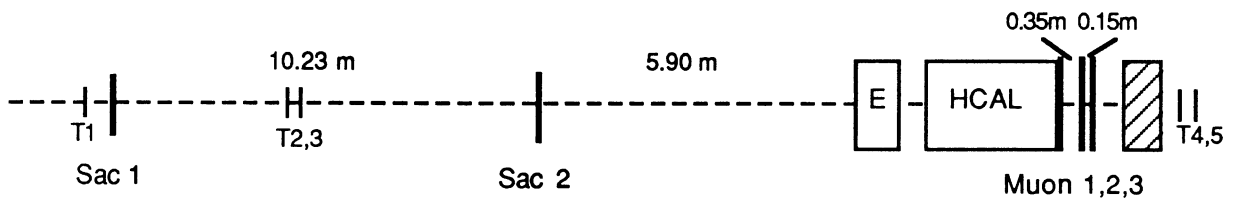


Figure 1

a) Top view

b) Side view (section)



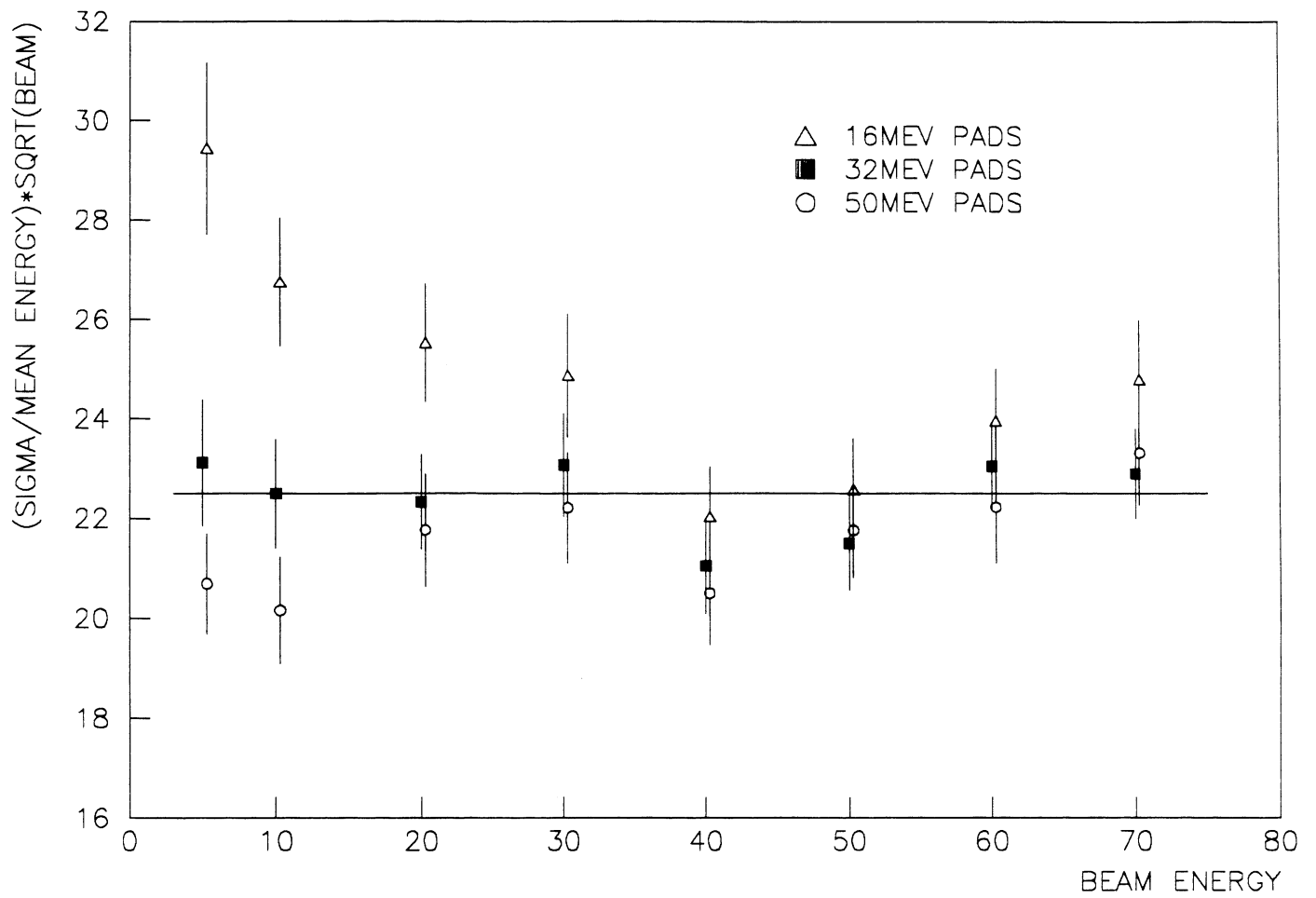


Figure 2 ECAL electron energy resolution

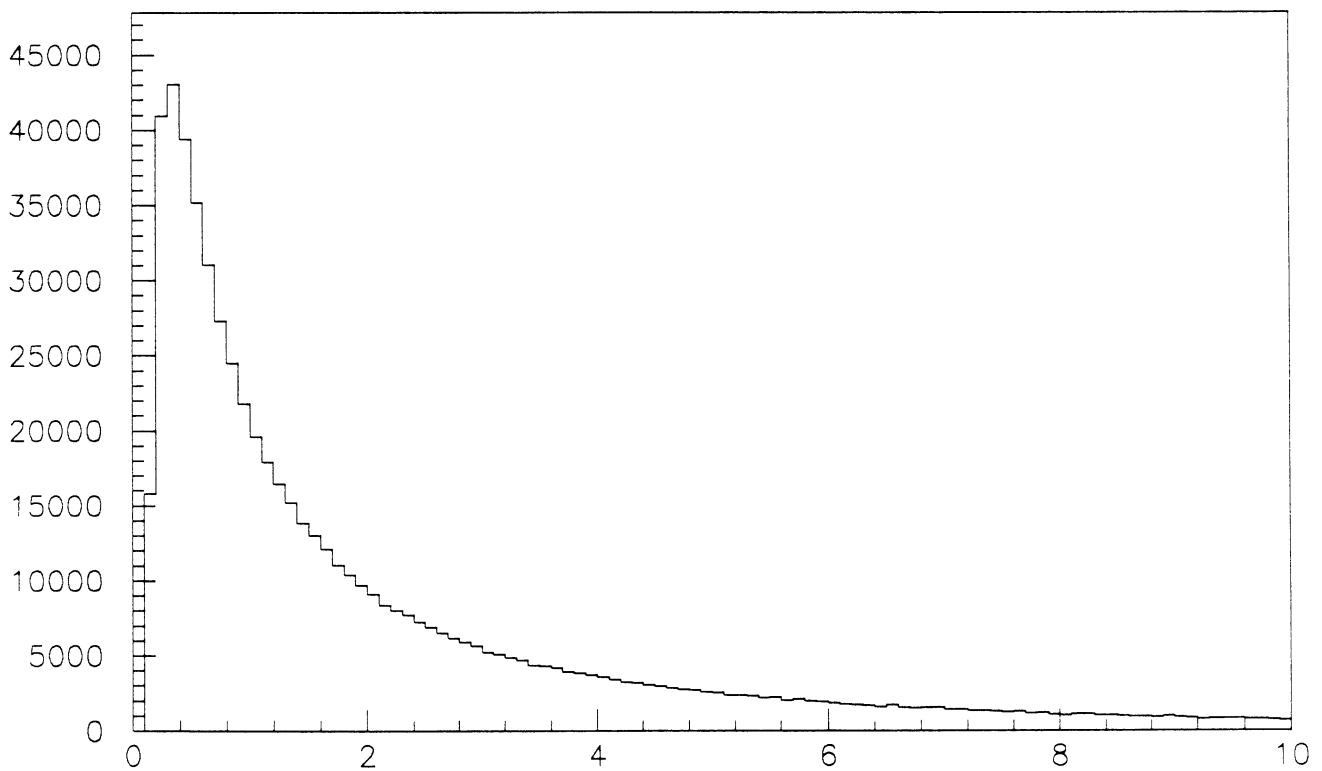


Figure 3 Energy distribution of Pions from LUND

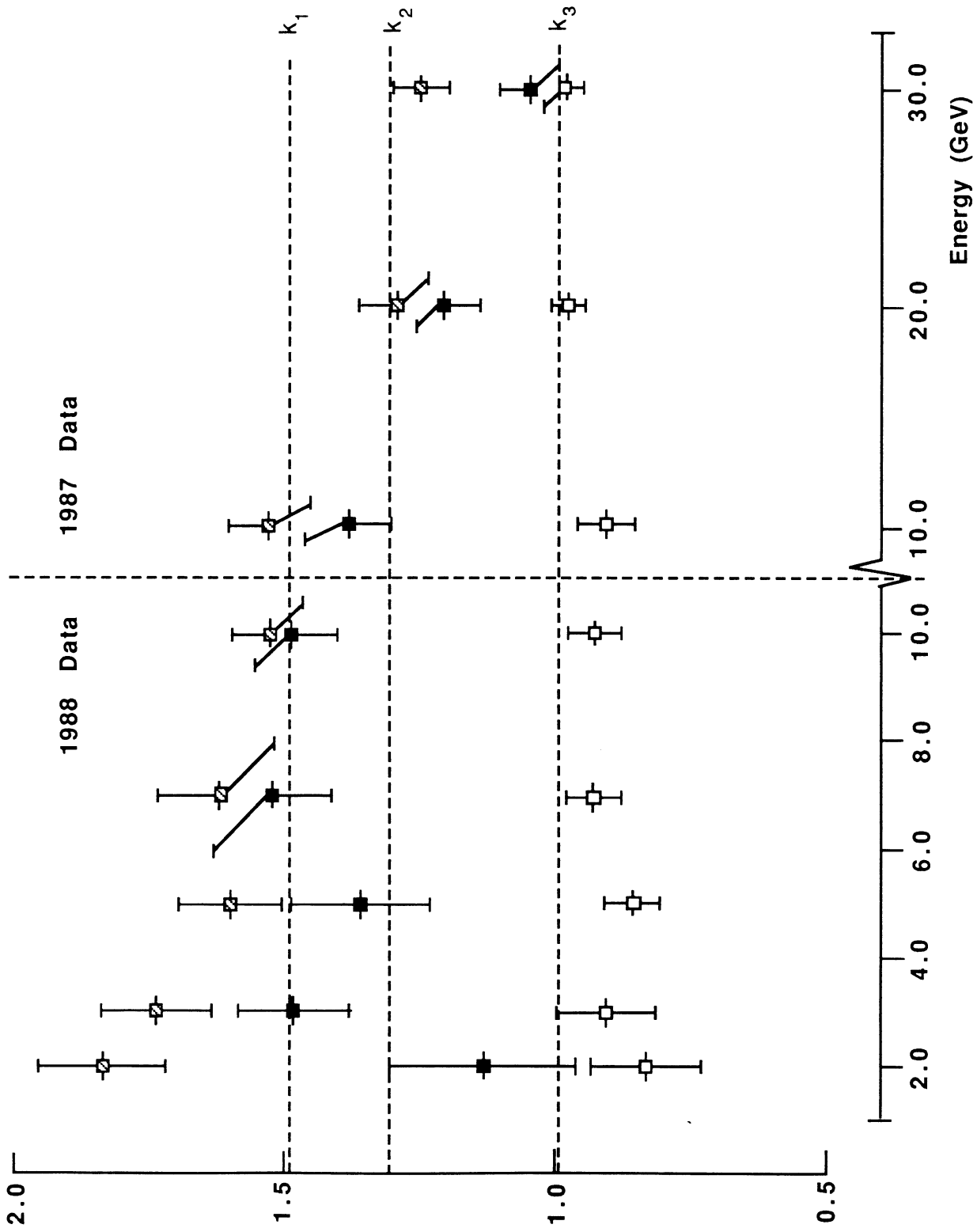


Figure 4 Variation of coefficients with energy

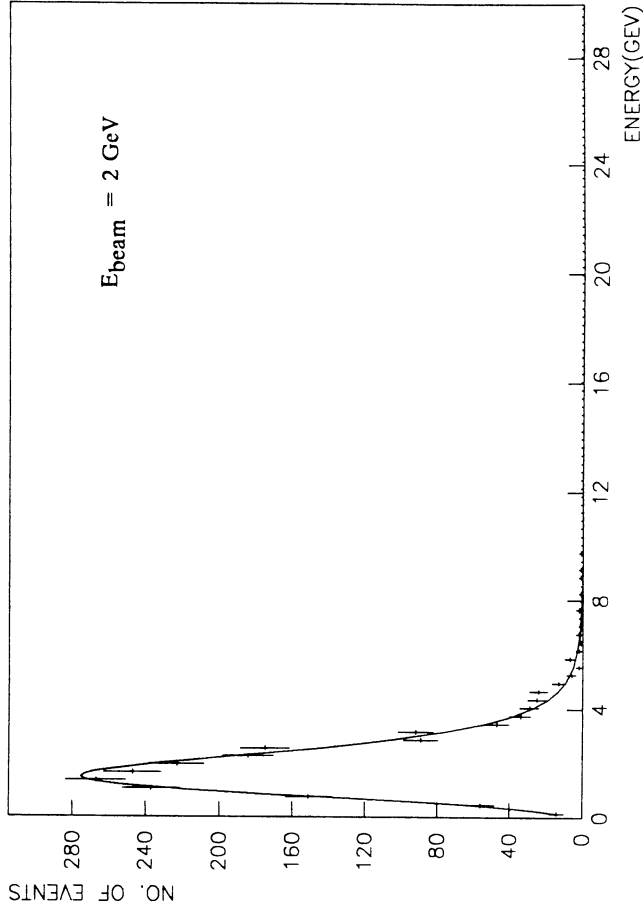
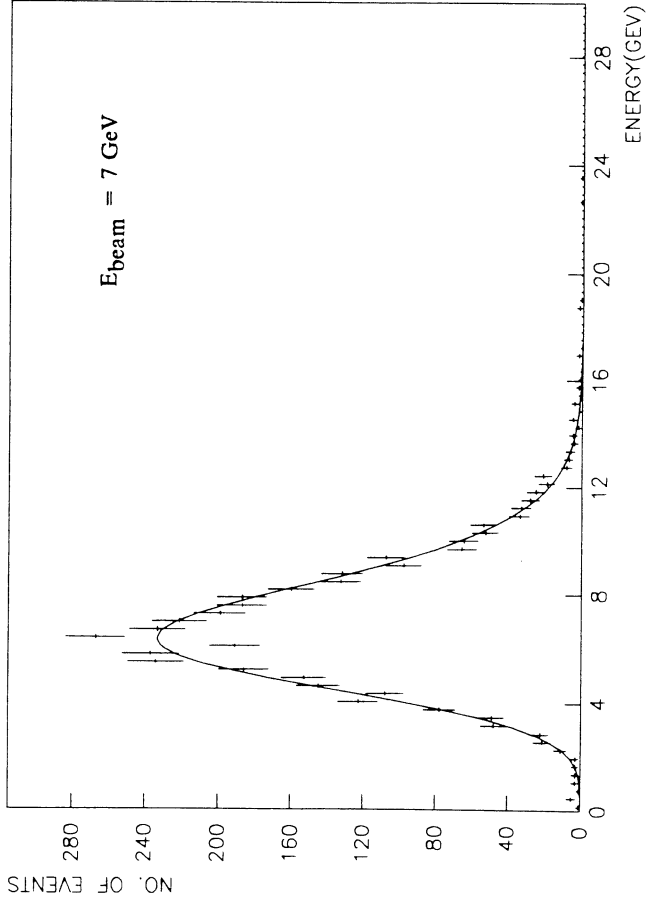
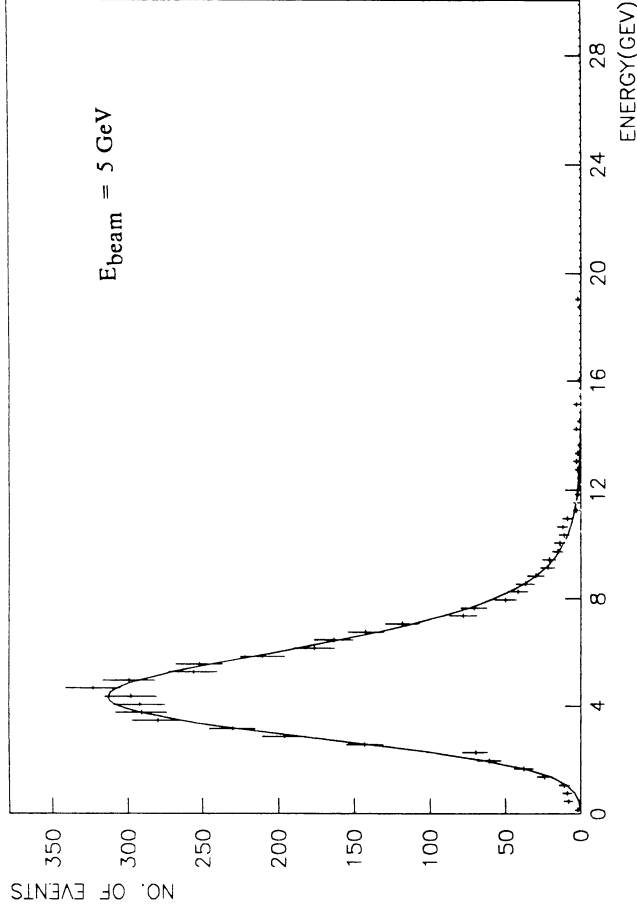
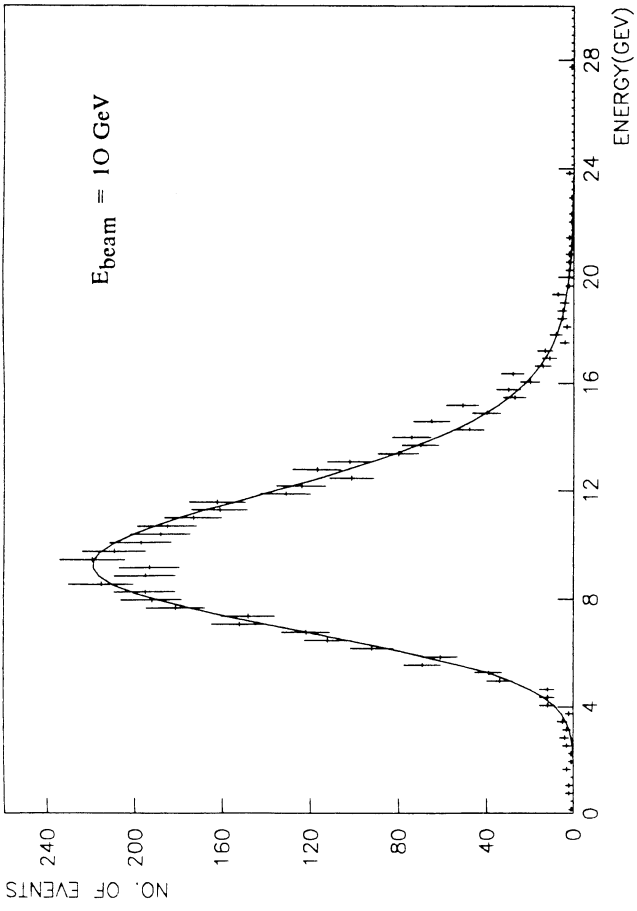
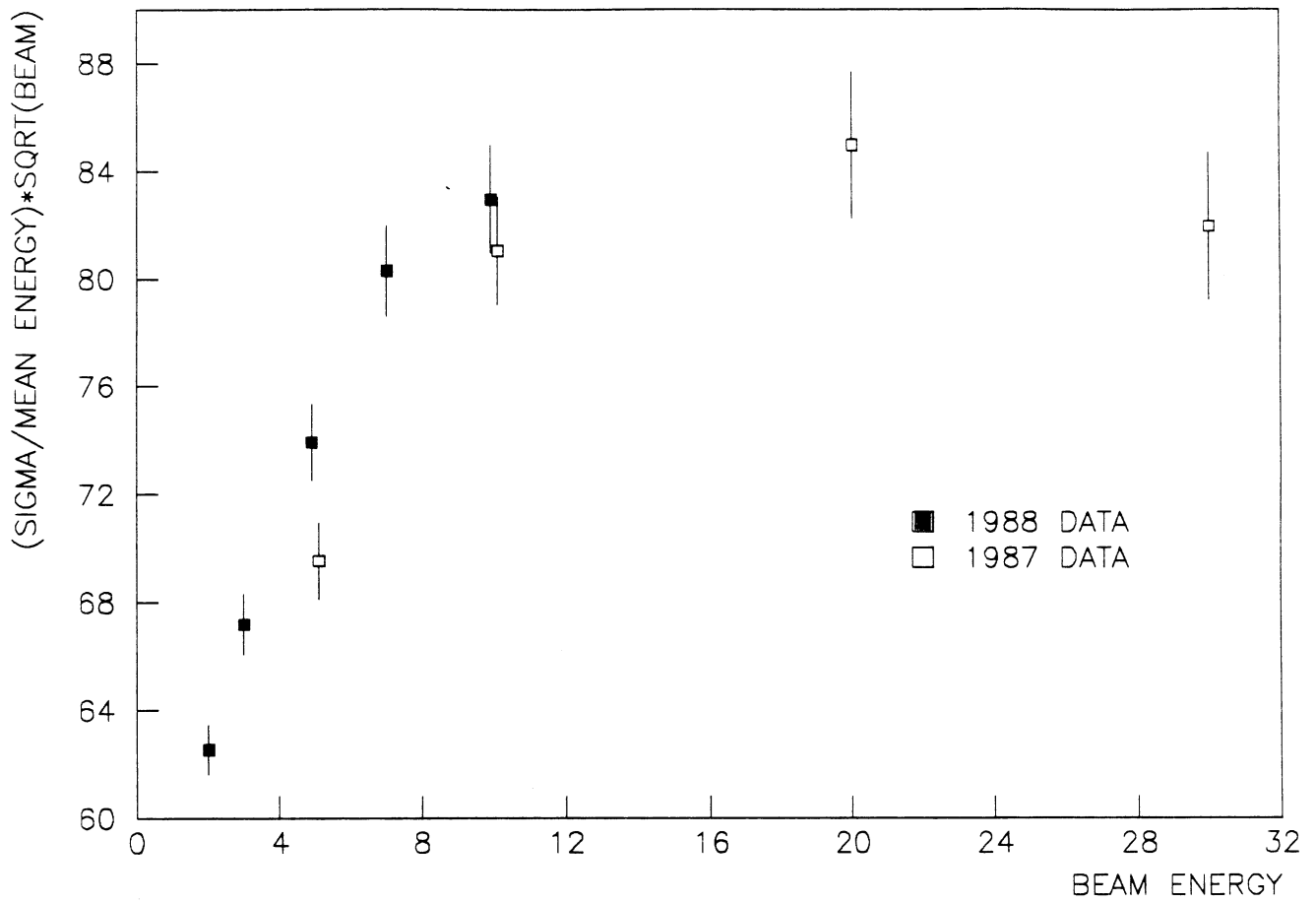


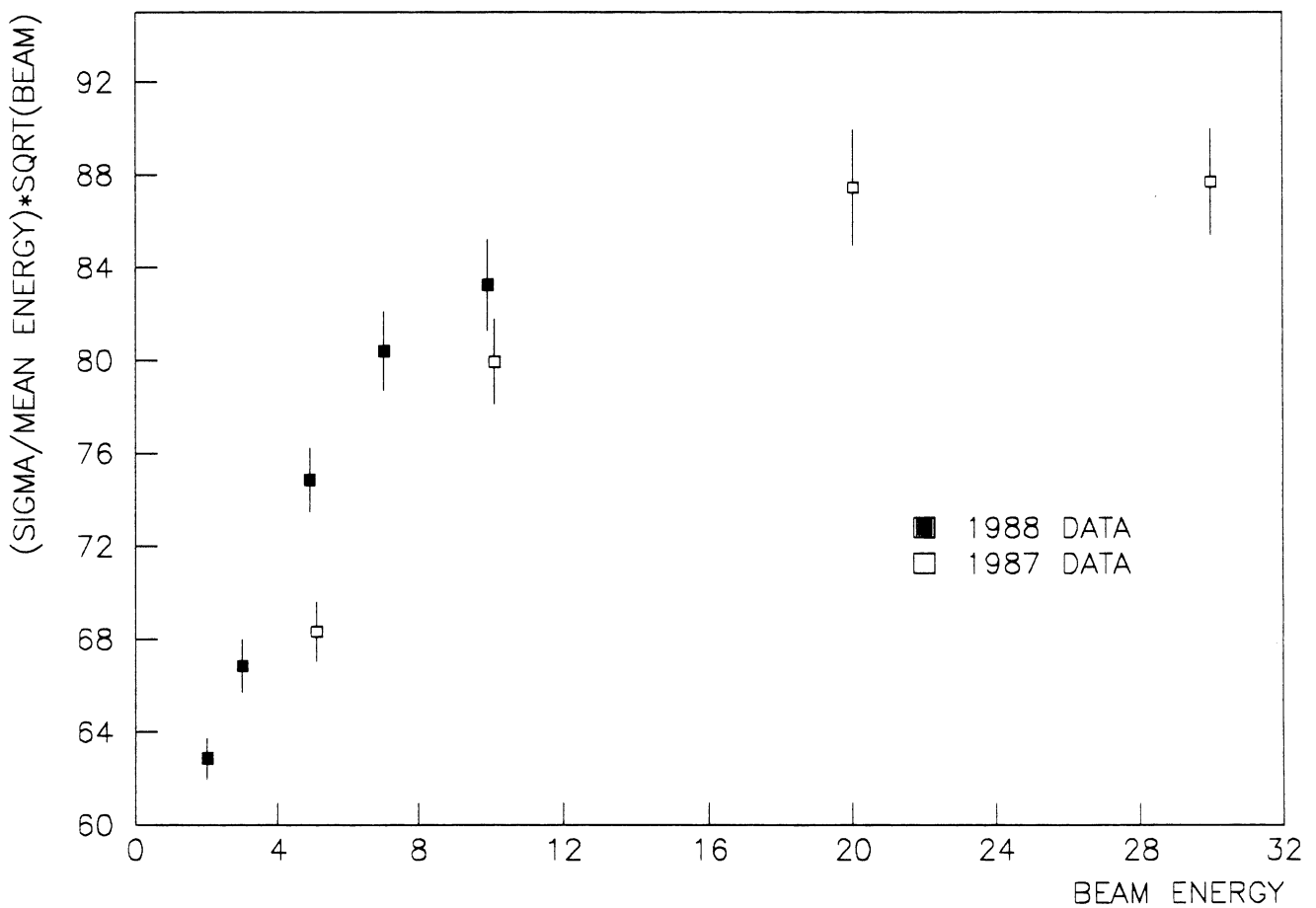
Figure 5 Measured distributions after minimisation

Figure 6 Energy resolution of combined calorimeter,

a) using individually minimised coefficients



b) using global coefficients



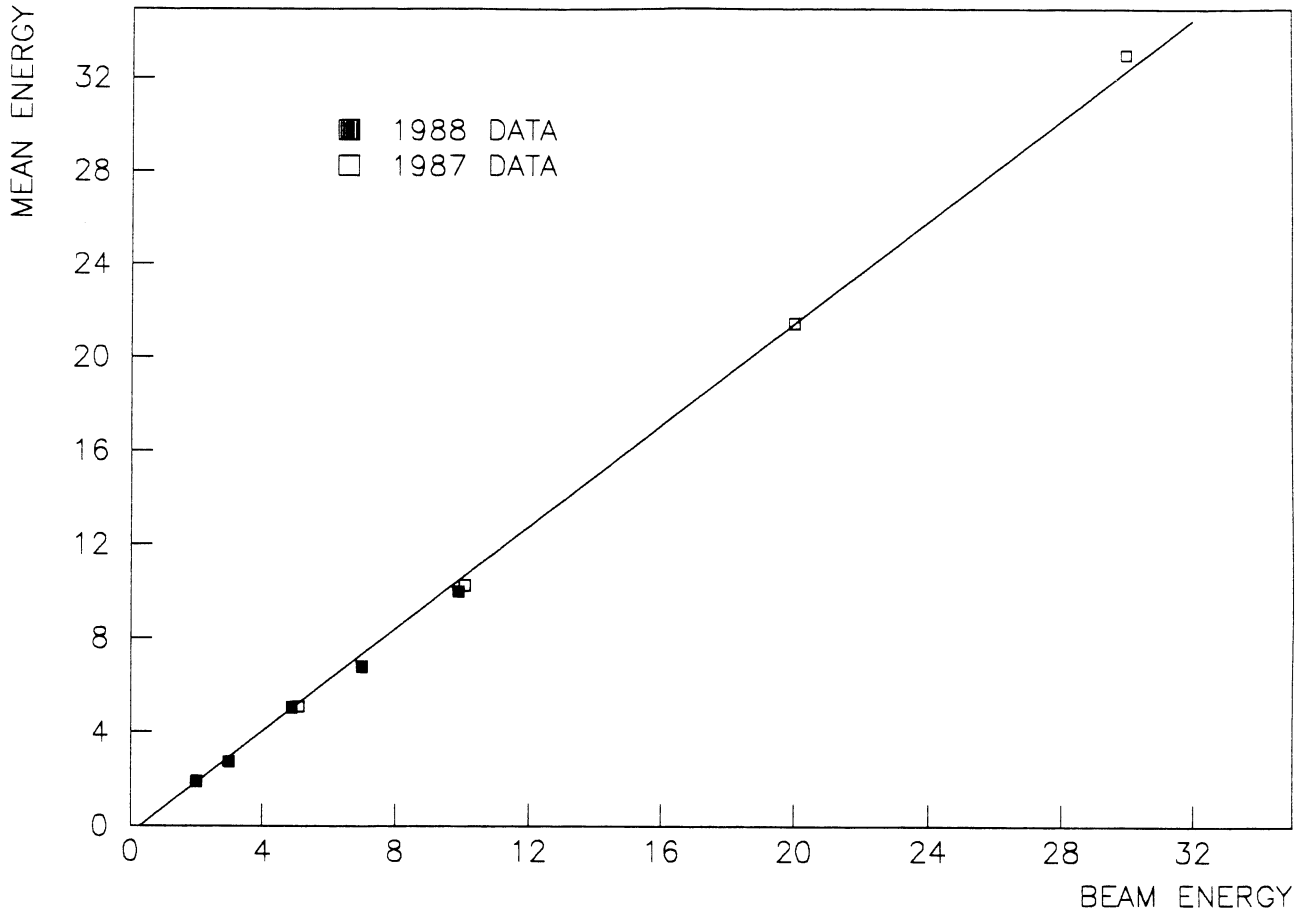


Figure 7 Linearity of energy measurement

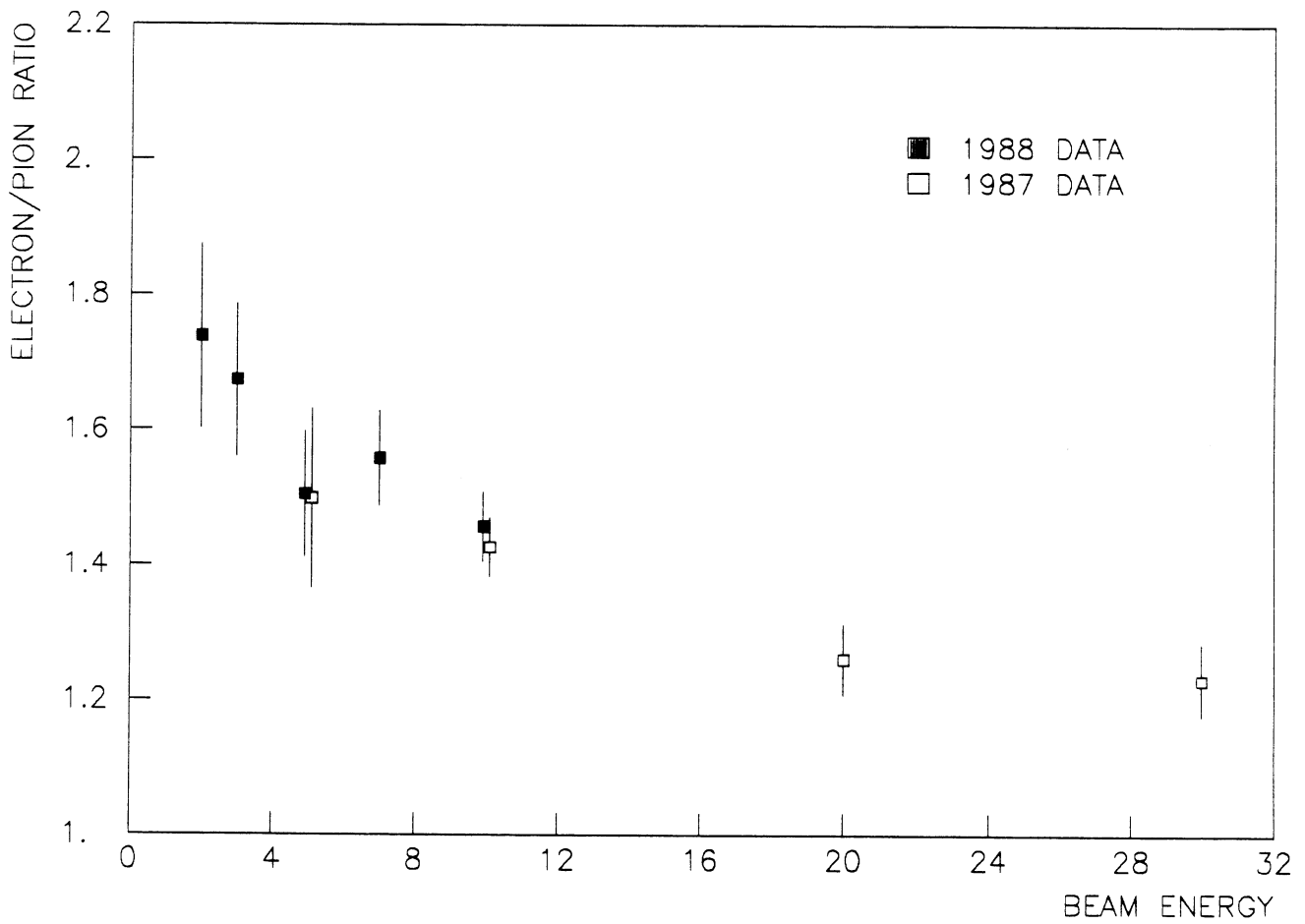


Figure 8 Electron to pion response ratio

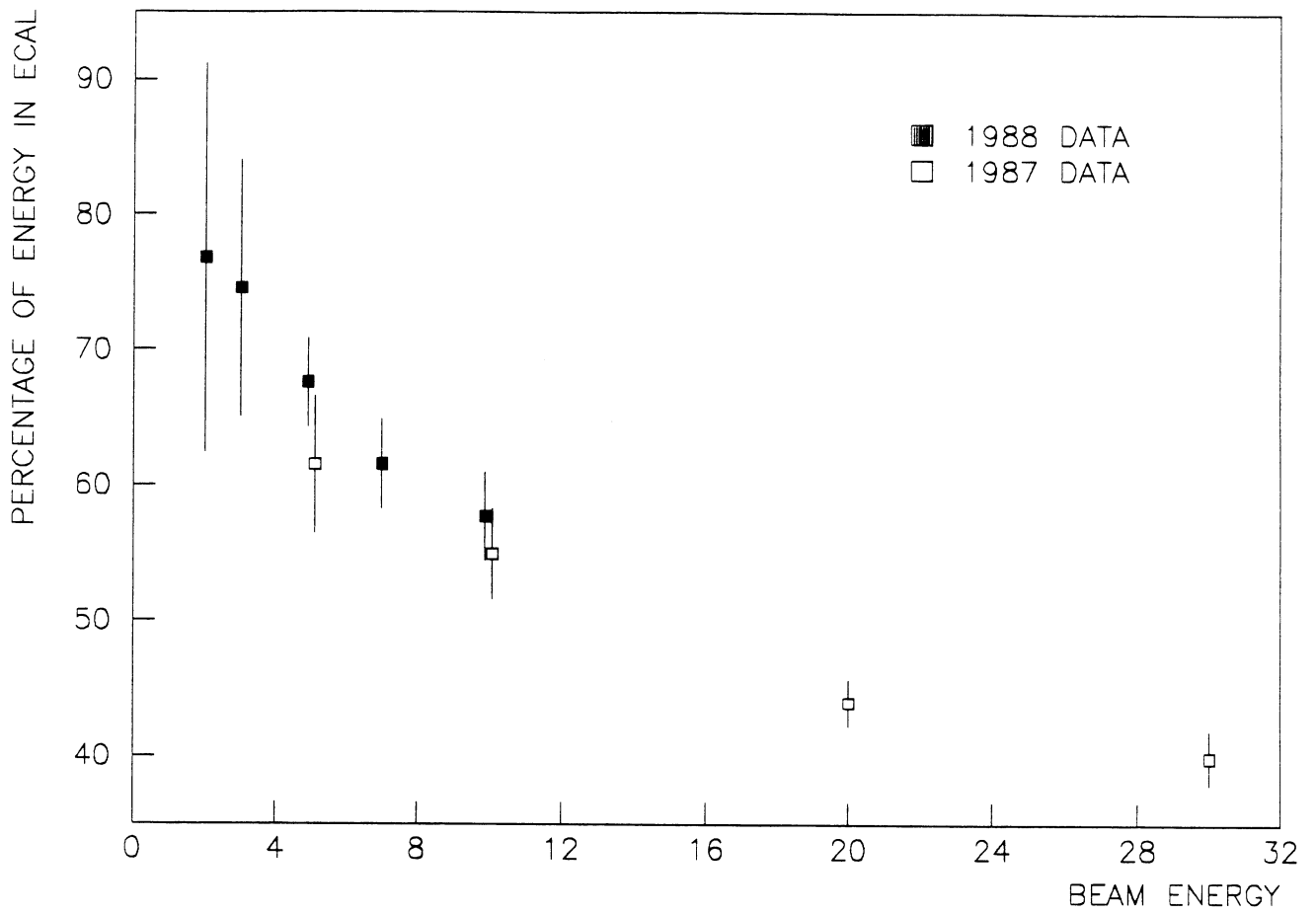
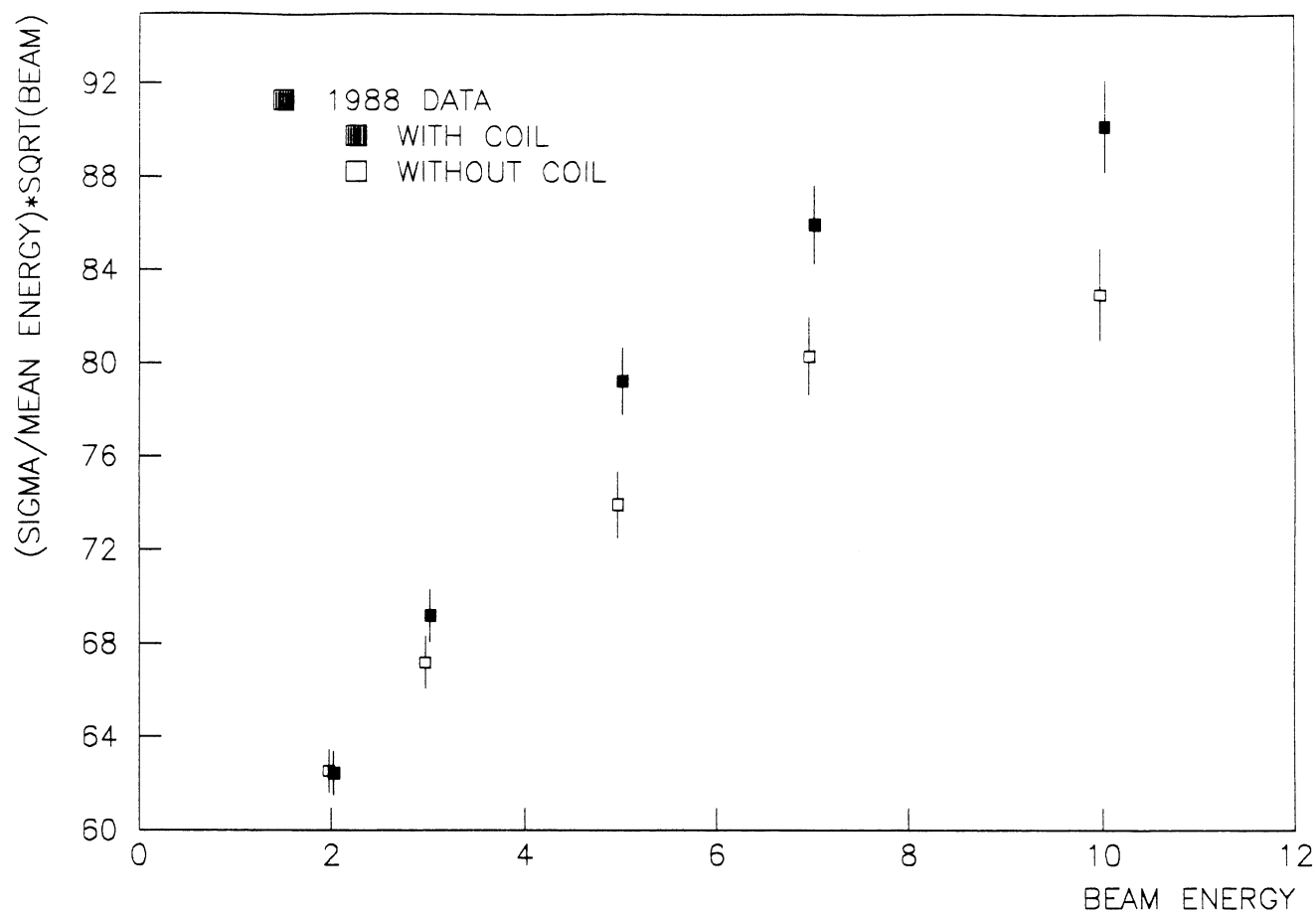


Figure 9 Fraction of energy in ECAL

Figure 10 Effect of the presence of the coil material on the :

a) Energy resolution of combined calorimeter



b) Linearity of the combined calorimeter

